AN R-BASED OVERVIEW OF THE WRW CONCEPT

Panagiotis Doulgeris[a], Araz Mahdad[a], Gerrit Blacquière[a]

[a]Department of Geotechnology, Delft University of Technology, The Netherlands

Contact author: Panagiotis Doulgeris, Department of Geotechnology, Delft University of Technology, Stevinweg 1, PO-Box 5048, 2628CN Delft, The Netherlands. Fax: +31 (0)15 27 81356, email: P.Doulgeris@TUDelft.nl

Abstract: *The WRW model serves the geoscientists' community as a global language dedicated to deliver a better insight into the seismic reflection experiment. The model formulates such an experiment as a multiplication of matrices. In today's numerical modeling, wave equation-based techniques such as implemented in the WRW model are used more and more, while it becomes clear that ray tracing methods do not have the required accuracy. The reflectivity matrix R is undoubtedly one of the most essential parts of the WRW model since it contains the angle dependent reflectivity information of the subsurface structures. It is this information that is to be retrieved from the seismic experiment. This paper provides insight in the formation process of this matrix. Different properties of the reflectivity matrix are investigated through the numerical modeling of three different cases. Moreover, the accuracy of the WRW approach is compared to that of ray tracing. The numerical results highlight the superiority of the WRW approach, i.e., the wave theory based approach, particularly in the case of a laterally variant reflector.*

Keywords: *WRW, reflectivity matrix, forward modeling*

1. INTRODUCTION

The main goal of the seismic reflection experiment is to obtain reflectivity information of subsurface structures. This can be done by means of structural imaging and reflectivity inversion processes on the acquired seismic data. Therefore, the forward modeling algorithm has a crucial impact on the inversion output. Among numerical modeling techniques, wave equation based modeling algorithms such as wave field extrapolation, and ray tracing are well

known. The WRW model, as introduced in [1], provides an efficient way to describe and handle mathematically the inversion parameters.

In the ray tracing approach, each ray path represents a seismic wave-front from a source to a receiver [2]. As the ray reaches an interface a part of it is transmitted and the rest is reflected depending only on the local reflectivity properties and the angle of incidence. As a result, the effect of irregularities on the reflectors cannot be properly taken into account [3].

On the other hand, according to the wave field extrapolation approach, wave propagation can be described by the contribution of secondary sources placed along the spherical wave front (Huygens' Principle). Therefore, in order to obtain the reflectivity information at a certain grid point on the reflective interface, the effect of neighboring grid points is also taken into account. Fig. 1 schematically represents the difference between the two methods. Wave field extrapolation based modeling can be described by means of the WRW model [1].

In this paper the WRW model will be analyzed with special attention given to the reflectivity matrix. 2D numerical examples will be presented and the results obtained from the two methods will be compared. The R matrices of the examples shall give an insight into the reflection mechanism and its impact on the final dataset. Finally, the deficiencies of the ray tracing approach with respect to the WRW approach will be discussed.

2. THE WRW MODEL

The key feature of the WRW model is that it describes the seismic data in terms of matrix operators in the frequency domain [1]. According to this model, each monochromatic component (single frequency) of the primary wave field $\mathbf{P}(z_0,z_0)$ that is recorded at the surface z_0, can be described in the space-frequency domain by:

$$\mathbf{P}(z_0,z_0)=\mathbf{D}(z_0)\sum_{m=1}^{M}[\mathbf{W}(z_0,z_m)\mathbf{R}(z_m,z_m)\mathbf{W}(z_m,z_0)]\mathbf{S}(z_0)\,. \tag{1}$$

In eq. 1, z_m denotes the steps in depth of the algorithm, thus, the depth levels that are investigated for reflective boundaries. The designation 'WRW model' stems from the two propagation matrix - operators **W**, and the matrix operator **R**, whose functions are explained below. It is worthwhile to mention that the WRW concept serves also as the vehicle for the CFP technology [4]. Fig. 2a shows a schematic representation of the WRW model.

The lateral coordinates x and y and the frequency ω have been left out for convenience.

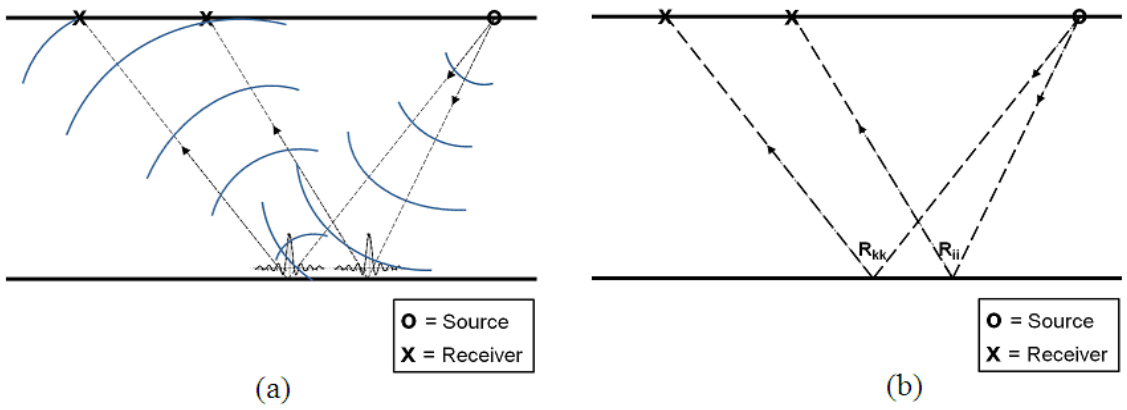

Fig.1: Different approaches to the reflection problem. (a) Wave theory (b) Ray tracing

The matrix operators in eq. 1 have the following meaning:

- $\mathbf{S}(z_0)$: source matrix. It contains the amplitude and phase of the source wavelet at the frequency under consideration. One column represents one source (array) and determines its position in space
- $\mathbf{W}(z_m, z_0)$: forward wave field propagation matrix. Each column contains a discrete version of the Green's function that describes the wave propagation from one point (one lateral location) at the surface z_0 to many points at depth level z_m.
- $\mathbf{R}(z_m, z_m)$: reflectivity matrix. It describes the conversion of an incident wave field into a reflected wave field, as will be further explained below.
- $\mathbf{W}(z_0, z_m)$: forward wave field propagation matrix. It describes the wave propagation from one point at the depth level z_m to many points at the surface z_0.
- $\mathbf{D}(z_0)$: detector matrix. It contains the detector wavelet. One row represents one detector (array) and determines its position in space.

It follows that the element $\mathbf{P}_{ij}$ of the *data matrix* $\mathbf{P}(z_0, z_0)$ corresponds to the configuration: source at the location j and detector at the location i. Therefore, one column of the data matrix represents a common source gather (shot record) and one row represents a common receiver gather. Other data gathers, such as CMP gathers or common offset gathers, can also be identified in the data matrix. This equation is valid for stationary acquisition geometries and stationary parts of non-stationary acquisition geometries.

3. REFLECTIVITY MATRIX

In the previous section, the general description of the WRW model was reviewed, in which the reflectivity matrix **R** was introduced as a matrix in the space-frequency domain containing operators that convert the incident wave field into the reflected wave field. These operators can be derived from the reflectivity operator in the wavenumber-frequency domain. In the case of a horizontal reflector between two homogeneous media it is given by [5]:

$$R(k_x, z_1, z_1, \omega) = \frac{\rho_2 k_{z,1} - \rho_1 k_{z,2}}{\rho_2 k_{z,1} + \rho_1 k_{z,2}}, \tag{2}$$

$$k_{z,(1,2)} = \sqrt{k_{1,2}^2 - (k_{1,2} \sin \alpha_{i,t})^2}, \tag{3}$$

where $\rho_{1,2}$ denotes the density of the two media and k_z is the z-axis component of k - the wavenumber (as shown in eq. 3). By $\alpha_{i,t}$ we denote the angle of incidence and angle of transmission respectively.

The reflectivity matrix **R** is a convolution matrix based on the operator R (eq. 1): the multiplication by R in the $k_x - \omega$ domain can be expressed in terms of a matrix multiplication by **R** in the $x - \omega$ domain. Fig. 2b represents schematically the formation of a convolution matrix from an operator. Each row of the reflectivity matrix $\mathbf{R}(z_m, z_m)$ contains an operator in the space-frequency domain which corresponds to a certain grid point at depth z_m.

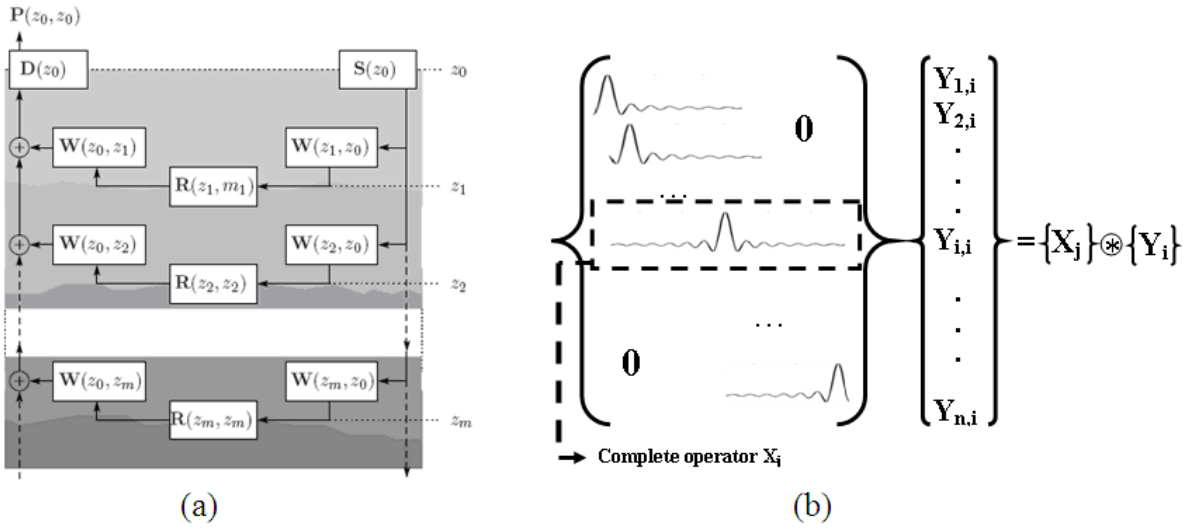

Fig. 2: (a) The WRW model, after the formulation of equation 1. For each reflection, a WRW-term is added to the total expression for the measured pressure $\mathbf{P}(z_0,z_0)$*, (b) Forming a convolution matrix*

In the simple case that all grid points at a certain depth have the same reflective properties (i.e. no lateral changes), the reflectivity matrix has a Toeplitz structure.

The angle dependent properties of the reflectivity operator are obtained from eq. 2 and 3. From eq. 3 it follows that each value of the reflectivity operator in the wavenumber - frequency domain represents reflectivity for a certain angle of incidence [6]. Two extreme cases are:

- Only diagonal elements of the reflectivity matrix are filled with non-zero values. In this case, the operator is constant over a range of wavenumbers, thus angles (angle independent reflector). In this case the grid points are treated as point diffractors.
- Constant values along the columns of the reflectivity matrix. In this case, the reflectivity operators in the wavenumber domain are non-zero for $k_x = 0$ only. Therefore, the grid points on the reflector reflect only the horizontal plane waves. One should note though that this is not a realistic situation.

In general, the matrix **R** is completely filled with various complex values. Note that the diagonal elements represent $x = 0$ (i.e. the grid-point under consideration). From Fourier theory it follows that this corresponds to a summation over the wavenumbers (or angles). Therefore, the diagonal elements of the reflectivity matrix represent angle-averaged reflectivity. Angle-averaged reflectivity is the result the many migration algorithms deliver, hence the importance of the diagonal elements of **R**. The off-diagonal elements of **R** contain information related to the angle-dependency of the reflectivity.

4. NUMERICAL EXAMPLES

The main aim of this section is to illustrate - through numerical examples - the properties of WRW wave equation modeling compared to those of ray tracing, as well as to analyze angle dependent reflectivity. Therefore, a number of simple, 2-D numerical examples have

been modeled. The velocity model consists of a single horizontal reflector at the depth of 100 m that forms the boundary between two media. Different cases will be considered with different medium properties. In all cases, the velocity is laterally invariant whereas density may vary along the reflector. The acquisition geometry consists of a 1.5 km long aperture with 5 m receiver spacing and a single source in the middle of the array. Medium properties for the different cases are listed in Table 1.

Configuration	ρ_1 (kg/m^3)	ρ_2 (kg/m^3)	c_1 [m/s]	c_2 [m/s]
Case 1	1500	2200	2000	3500
Case 2	2000	1000	2000	2500
Case 3	1000-3500	1000-3500	2000	2200

Table 1: Medium properties of different cases studied

4.1. Case 1 – Homogeneous media

As shown in Table 3.1, the medium properties in case 1 refer to the simple situation of two homogeneous layers with layer 2 having a higher acoustic impedance than layer 1. Therefore, all the grid points on the reflector have the same impedance contrast, hence, the same reflectivity operator in the wavenumber domain (homogeneous reflector). Fig. 3a and 3b show the shot records obtained from WRW and ray tracing modeling, respectively. Due to the simple properties of the reflector, no significant difference can be observed in the modeled shot records between the two methods. Fig. 3c displays the absolute value of the reflectivity operator in the wavenumber-frequency (k_x, ω) domain. As illustrated in this figure, three different areas are clearly separated by dipping boundaries.

- The central turquoise area corresponds to reflection angles of incidence from 0^o (i.e. vertical incidence) up to the critical angle.
- The second, red, area consists of post-critical angles up to 90^o. For these angles total reflection occurs, thus, the reflectivity values are close to 1.
- The last, blue, area corresponds to reflectivity over 90^o and refers to the evanescent part of the reflected wave field. More information on evanescent wave fields can be found in [5].

The angle dependent reflectivity can be better observed in Fig. 3d in which the real part and the absolute value of the reflectivity are depicted as a function of angle of incidence. The real part of the reflectivity reaches its minimum for 0^o angle of incidence and its maximum value at critical angle. It collapses after the critical angle, while the absolute value remains 1 till 90^o. Fig. 3e shows the reflectivity matrix R with dominant diagonal elements which represent angle-averaged reflectivity, as mentioned before.

4.2. Case 2 – Homogeneous media & polarity reversal effect

In this case, the bottom layer has lower acoustic impedance than the upper layer. Therefore, one expects to have a negative reflection coefficient. However, in this specific situation, the angle dependency plays an essential role in the simulated output.

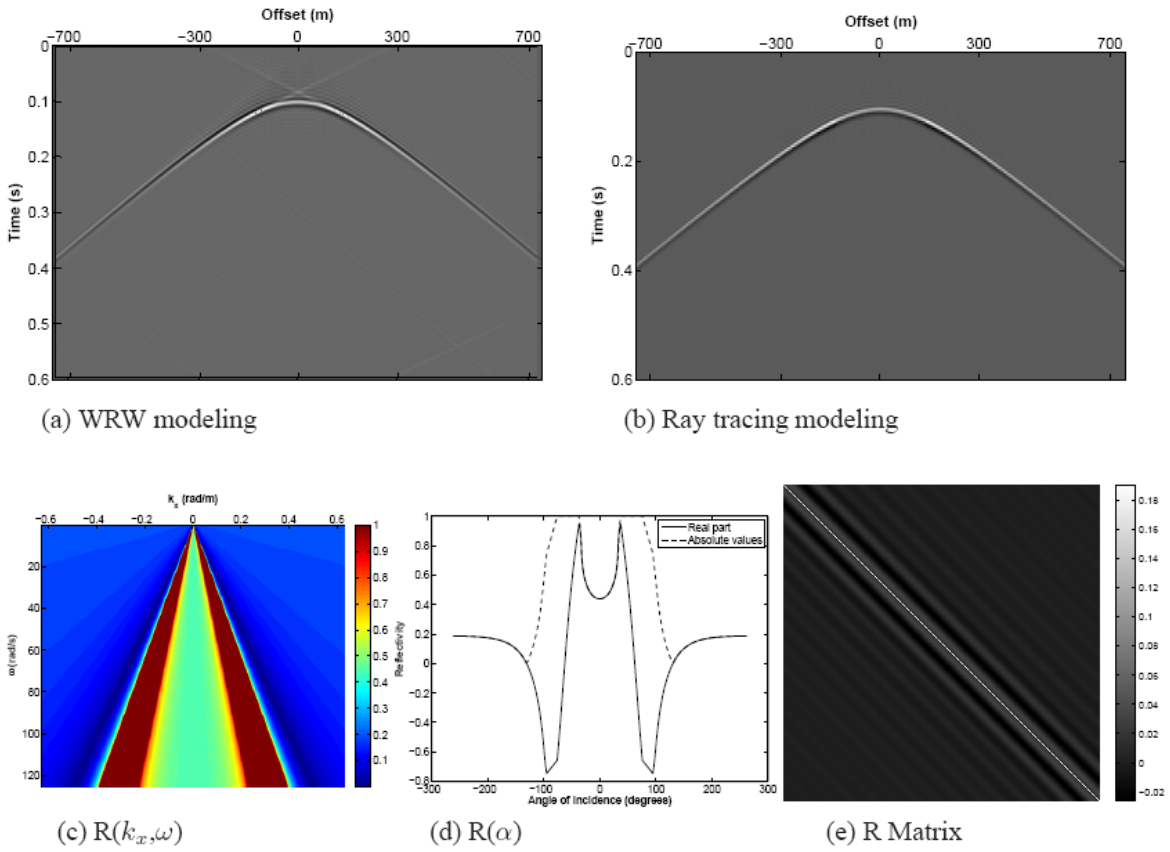

Fig. 3: Shot records obtained by the WRW modeling (a) and the ray tracing approach (b) for case 1. Different forms of the R operator follow: (c) in the $k_x - \omega$ domain, (d) versus angle and (e) the actual image of the reflectivity matrix as used in the WRW formulation.

It even causes the reflection coefficient to change its polarity as the angle of incidence increases. This is illustrated in Fig. 4a and 4b for the WRW model and the ray tracing method respectively. For narrow offsets (small angles), the reflector has a negative polarity. The amplitude goes smoothly to zero for further offsets and becomes positive again for larger offsets (larger angles), with a reversed, positive polarity. However, the range of offsets with very low amplitude is different for the two simulated results. The WRW modeling result displays a wider range of offsets with very low amplitude level. As illustrated, the reflectivity is negative for small angles; it becomes zero for a certain angle and then steeply reaches the critical angle. There is only a small difference between the angle at which zero reflectivity occurs and the critical angle.

4.3. Case 3 – Media with random density along the lateral direction

In this case the density is randomly varying between 1000 kg/m^3 and 3500 kg/m^3 along the top and the bottom of the boundary but the velocity remains laterally invariant in each layer. Therefore, the wave propagation in the upper medium remains simple. Because of the random density effect, low impedance contrasts may occur along the reflector. These produce the no-reflectivity gaps on the event in the case of ray-tracing, and the diffraction patterns in

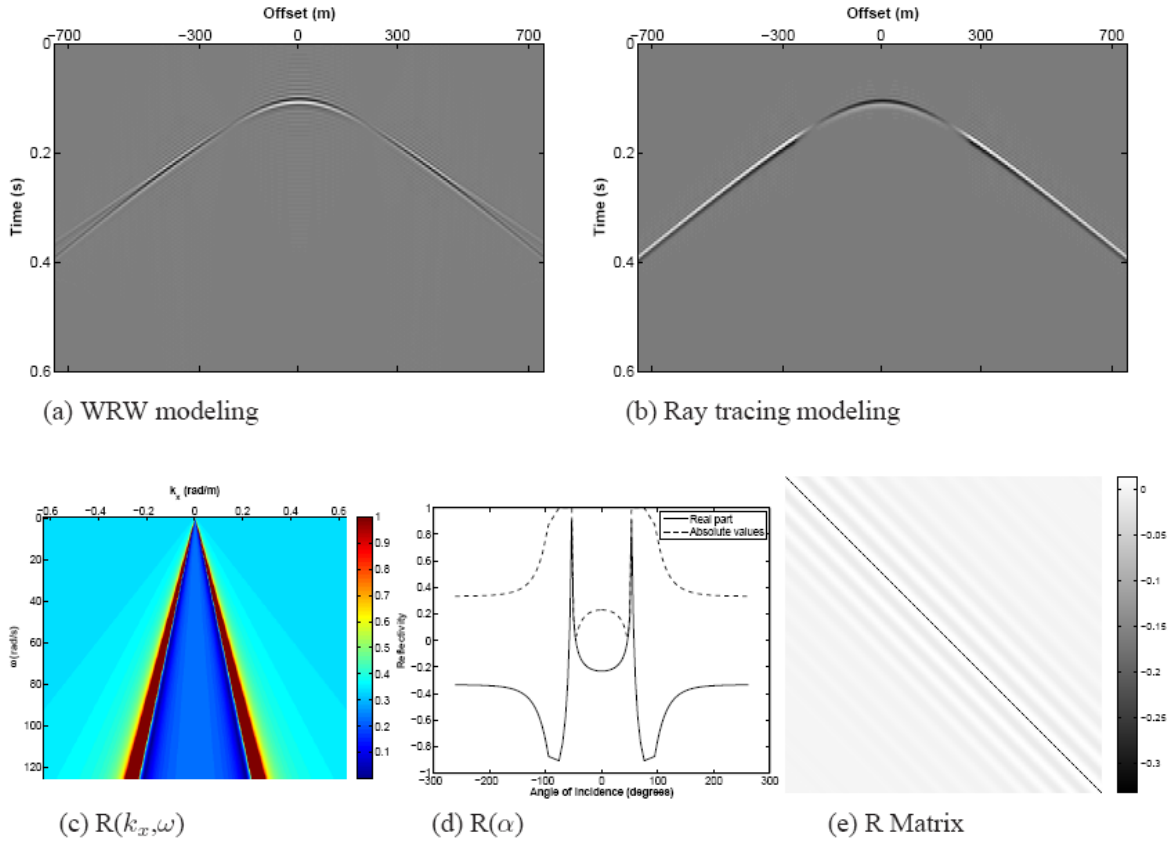

Fig. 4: Shot records obtained by the WRW modeling (a) and the ray tracing approach (b) for case 2. Different forms of the R operator follow: (c) in the kx − ω domain, (d) versus angle and (e) the actual image of the reflectivity matrix as used in the WRW formulation.

the case of wave equation modeling. By comparing Fig. 5a and 5b, it can indeed be seen that diffraction patterns due to the irregularities in the reflector are not included in the simulated result obtained by ray tracing, since each grid point on the reflector is treated individually. This example illustrates that the wave equation approach is clearly preferred in this case.

5. DISCUSSION AND CONCLUSION

In this paper, the reflectivity matrix in the general context of the WRW model is studied and different examples are provided to highlight its properties as well as its effect on the final shot record. The general frame of this study consists of the modeling of a horizontal reflector based on two different approaches, the wave equation approach (using the aforementioned reflectivity matrix) and the ray tracing approach. Differences between the outcome of these two methods comprise the limitations of ray tracing, while pointing out the virtues of the WRW concept. As shown in Fig. 1(a), the essence of the wave equation approach is that the reflectivity matrix acts as a spatial convolution operator on the downgoing wave field. On the contrary, ray tracing only applies an amplitude coefficient on each ray. Fig. 5a and 5b illustrate characteristically the outcome. The **R** matrix, applied on the wave field in the spatial domain, produces a main uninterrupted event with diffraction patterns due to the random lateral density variations that are present in this case. On the other hand, the ray tracing

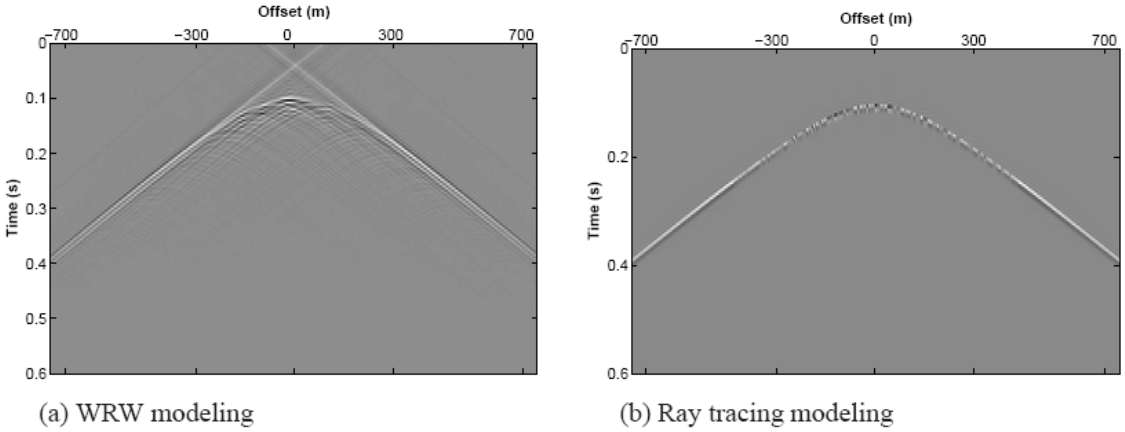

Fig. 5: Shot records obtained by the WRW modeling (a) and the ray tracing approach (b) for case 3.

technique fails to model these diffraction patterns, as it is based on the local impedance contrast at each grid point. Hence, non-realistic gaps are produced on the reflection event.

In conclusion, the distinguishing features of the wave theory modeling (WRW approach) appear when there is irregularity or variability in the subsurface structures, especially in the lateral direction. This situation happens often in reality and ray tracing is unable to invert correctly for amplitudes during the migration process. This example illustrates once more the importance of wave equation based modeling.

REFERENCES

[1] **Berkhout, A. J.,** *Seismic migration, imaging of acoustic energy by wave field extrapolation*, Elsevier, Amsterdam, 1982.

[2] **Grunberg, M. D., Genaud, S., and Mongenet, C.,** Seismic ray-tracing and earth mesh modeling on various parallel architectures, *The Journal of Supercomputing,* volume 29, No 1, pp. 27 – 44, 2004.

[3] **Berkhout, A. J., de Vries, D., Baan, J., and van den Oetelaar, B. W.,** A wave field extrapolation approach to acoustical modeling in enclosed spaces, *Journal of Acoustical Society of America,* Volume 105, Issue 3, pp.1725-1733, 1999.

[4] **Thorbecke, J. W.,** *Common Focus Point technology: Ph.D. thesis,* Delft University of Technology, pp. 35 – 50, 1997.

[5] **Wapenaar, C. P. A., and Berkhout, A. J.,** *Elastic wave field extrapolation: redatuming of single- and multi-component seismic data,* Elsevier, pp. 96 – 98, 1989.

[6] **van Veldhuizen, E. J., Blacquière, G., and Berkhout, A. J.,** Acquisition geometry analysis in complex 3D media, *Geophysics,* volume 73, No. 5, pp. Q43–Q58, 2008.